Research Article

Monalisa Anand*, Palla Danumjaya, and Ponnada Raja Sekhara Rao

Influence of incubation delays on COVID-19 transmission in diabetic and non-diabetic populations – an endemic prevalence case

Abstract: The study of dynamics of diabetic population infected by COVID-19 is of pressing concern as people with diabetes are considered to be at higher risk of severe illness from COVID-19. A three-compartment mathematical model to describe the interactions of diabetic population and non-diabetic population both infected by COVID-19 with a susceptible population is considered. Time delays in incubation periods of COVID-19 in diabetic and non-diabetic populations are introduced. Besides the basic properties of such a dynamical system, both local and global stability of endemic equilibrium, are studied. The lengths of time delays are estimated for which the stability of the system is preserved locally, while sufficient conditions on system parameters are obtained for global stability. Numerical examples are provided to establish the theory, and simulations are provided to visualize the examples. It is noted that an increase in length of time delay in either of infected populations leads to oscillations in susceptible population but has no impact on infected populations.

Keywords: COVID-19, diabetes, delay differential equation, equilibria, stability analysis, numerical experiments

MSC 2020: 92C42, 93C43, 92D25

1 Introduction

COVID-19 is a highly infectious respiratory illness caused by the novel coronavirus, SARS-CoV-2, and it was first identified in Wuhan, China, in December 2019. The transmission of this disease is via contaminated air droplets or small airborne particles containing the virus. General symptoms include fever, cough, headache, fatigue, and loss of taste and smell, among many others. Individuals of all ages are at risk of contracting this infection; however, patients with age greater than 60 years with underlying medical condition have an increased risk of developing serious complications [6]. The most prevalent comorbidity of COVID-19 is hypertension (42.46%), followed by diabetes (39.72%), old k-chest (20.54%), bronchial asthma (16.43%), coronary artery disease (13.69%), chronic kidney disease (13.69%), and valvular heart disease (6.84%) [4]. Studies [5,8,11,29] have highlighted that COVID-19 patients with diabetes, cardiovascular diseases, hypertension, and other comorbidities are likely to develop a more severe course and progression of the disease, which could develop into a life threatening situation leading to death.

COVID-19 patients with diabetes experience significantly higher rates of complications and mortality [16,19,28]. Joshi and Pozzilli [16] emphasized on the COVID-19 induced diabetes, which is a novel phenomena

---

* Corresponding author: Monalisa Anand, Department of Mathematics, BITS-Pilani K.K. Birla Goa Campus, Goa-403726, India,
e-mail: monalisaanand066@gmail.com
Palla Danumjaya: Department of Mathematics, BITS-Pilani K.K. Birla Goa Campus, Goa-403726, India, e-mail: danu@goa.bits-pilani.ac.in
Ponnada Raja Sekhara Rao: Department of Mathematics, Govt. Polytechnic for Minorities, Guntur-522005, A.P., India,
e-mail: raoprs@gmail.com

observed in critically ill patients. COVID-19 patients with diabetes frequently experience uncontrolled hyperglycaemia and episodes of acute hyperglycaemic crisis, requiring exceptionally high doses of insulin [30]. COVID-19 has been associated with the development of new-onset hyperglycemia and worsening of glycemic control in pre-existing diabetes, due to direct pancreatic damage by the virus, body's stress response to infection, and use of diabetogenic drugs such as corticosteroids in the treatment of severe COVID-19 [35]. Diabetes is one of the major risk factors for fatal outcomes from COVID-19, and a 64% greater risk of diabetes was found in patients with COVID-19 [22]. Patients with diabetes are vulnerable to infection because of hyperglycemia and impaired immune function [15]. During the COVID-19 pandemic, diabetes care was also affected and had a negative impact on people with diabetes, as the healthcare providers were overloaded by COVID-19 cases [12].

Several studies [1,18,20,26,33] suggest a mathematical model to study the dynamics of the spread of COVID-19 in diabetic patients. Mathematical models have been used in literature since decades to examine, analyze, and predict future events and to bring the system to a desirable and controllable state. The real impact of mathematical modeling on public health came with the need for evaluating intervention strategies for newly emerging and re-emerging pathogens [21]. Hence, the study of the interaction between COVID-19 infection and diabetes to understand the spread of epidemic, as well as identification and control, is of utmost importance in current scenario. Kouidere et al. [20] suggested a mathematical modelling of the spread of the COVID-19 pandemic, highlighting the negative impact of quarantine on diabetic population. Khan et al. [18] proposed a first-order nonlinear mathematical model for hypertensive or diabetic patients open to COVID-19. Okyere and Ackora-Prah [24] suggested that more attention should be given to COVID-19 patients with diabetes as they have increased chance of death. Various mathematical modelling of COVID-19 disease has been done extensively in literature with or without comorbidities [2,23,25,31,32].

Our primary focus in this article revolves around examining the impact of COVID-19 on individuals with and without diabetes, incorporating incubation time delays in both populations. In our recent study [1], we developed a mathematical model that initially did not account for time delays. However, we acknowledge that in real-life scenarios, there is a period of time before symptoms of the infection manifest in the host's body, indicating that it is not an instantaneous process. Therefore, mathematical models utilizing delay differential equations are employed to address this limitation of ordinary differential equation (ODE) models. Delay differential equations involve time derivatives that depend on the solution at previous time points. Over the past few decades, the literature has seen an increased focus on the analysis and control of continuous-time delay systems. The main objective of the model presented in this article is to comprehend the dynamics of COVID-19 infection among individuals with and without diabetes, specifically examining the tolerable level of incubation time delay that allows the system to reach a desirable state.

The outline of the article is as follows: Section 2 introduces our mathematical model incorporating time delays, which represents the susceptible population, as well as the COVID-19-infected populations of both diabetic and non-diabetic individuals. We define the model parameters and derive the characteristic equation. Moving to Section 3, we explore the conditions under which the endemic equilibrium point will be locally stable, considering various scenarios of time delays. Section 4 focuses on the global stability of the endemic equilibrium point. In Section 5, we validate the theoretical results obtained in the previous sections through numerical experiments. Finally, we conclude with a discussion and provide insight into future prospects in the last section.

2 The mathematical model

We present a nonlinear delay mathematical model to study the transmission of COVID-19 infection in diabetic and non-diabetic population. We denote the total susceptible population by $x(t)$; the infected diabetic population by $y(t)$, and $z(t)$ denotes the infected non-diabetic population at time t. Here, we have introduced two different time delays in our model to study their consequences on the dynamic behaviour of the model. Below, we briefly discuss about the biological significance of these time delays.

- τ_1: The time delay $\tau_1 \geq 0$ has been incorporated to account for the presence of the incubation period of the COVID-19 virus specifically in the diabetic population. Thus, τ_1 represents the duration between infection and the activation or onset of COVID-19 symptoms in individuals with diabetes.
- τ_2: The delay $\tau_2 \geq 0$ takes into consideration the time delay in the onset of symptoms of COVID-19 in the non-diabetic population.

Figure 1 shows a pictorial representation of our model.

We consider the following system of delay differential equations:

$$\begin{aligned}
x'(t) &= f(x) - dx - af_1(x)y - bf_2(x)z + pa_1y + qa_2z, \\
y'(t) &= a_1 af_1(x(t - \tau_1))y + b_1 \beta f_2(x(t - \tau_2))z - d_1y - a_1y, \\
z'(t) &= a_1(1 - a)f_1(x(t - \tau_1))y + b_1(1 - \beta)f_2(x(t - \tau_2))z - d_2z - a_2z,
\end{aligned} \tag{2.1}$$

with initial populations

$$x(t) = \chi(t) > 0, y(t) = \zeta(t) > 0, z(t) = \eta(t) > 0, t \in [-\tau, 0], \tau = \max\{\tau_1, \tau_2\}.$$

In equation (2.1), $f(x)$ is the growth rate function of the susceptible population x, whereas f_1 and f_2 are the conversion functions of y and z, respectively. They are converting the susceptible population into infected ones after contact. We assume these functions to be non-negative, as they define the growth rate of the populations. Several examples of these types of functions are available in literature, such as $\frac{ax}{1+x}$ (Holling Type II) and $\frac{ax^k}{1+x^k}$ (Holling Type III). The model consists of three main variables, two time delays, and several parameters. These variables and parameters are important to capture the dynamics occurring in the transmission of COVID-19 among diabetic and non-diabetic groups in a certain population. Here, all the parameters are non-negative owing to the biological significance. The parameters d, d_1, and d_2 represent the specific death rates of the susceptible, infected diabetic, and infected non-diabetic populations. The death could be natural due to ageing, diseases, etc. for susceptible population, while it could be due to COVID-19 and its comorbidities for infected populations. Rest of the parameters are given in Table 1 for a clear understanding.

We assume that the functions f, f_1, and f_2 satisfy the local Lipschitz conditions, and hence, equation (2.1) has unique solutions that are continuable in their maximal intervals of existence for appropriate initial conditions [13]. Furthermore, following arguments as in the study by Rao and Kumar [27], one can see that
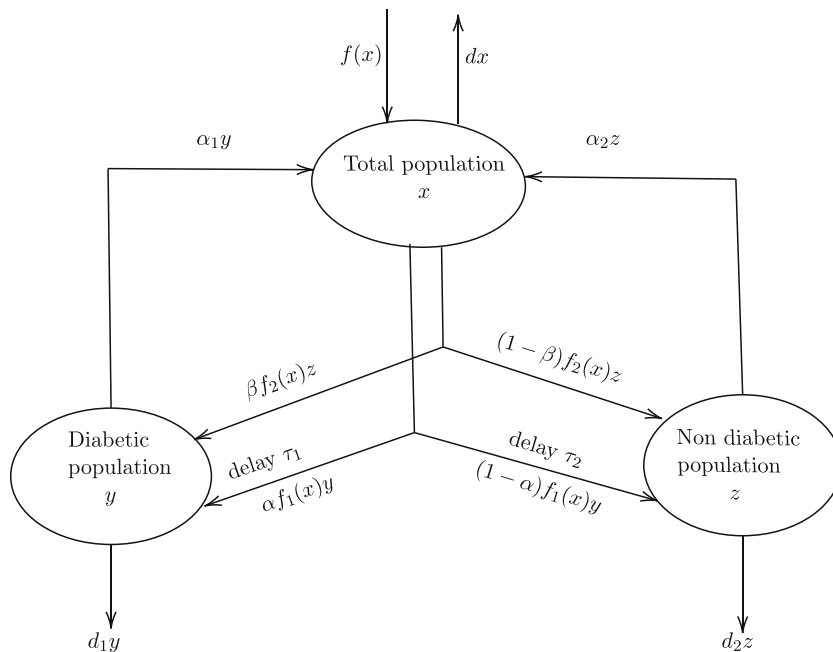

Figure 1: Schematic diagram of the proposed model.

Table 1: Notations of the model parameters with their biological significance

Parameters	Biological significance
a	Contact (exposure) rate of y with x
b	Contact (exposure) rate of z with x
a_1	Rate of infection of exposed y
b_1	Rate of infection of exposed z
α	Part of diabetic population infected by y
β	Part of diabetic population infected by z
α_1	Quarantine + treatment rate of y
α_2	Quarantine + treatment rate of z
p	Part of recovered population of y becoming susceptible again
q	Part of recovered population of z becoming susceptible again
d	Specific mortality rate of x
d_1	Specific mortality rate of y
d_2	Specific mortality rate of z

the solutions of equation (2.1) are also non-negative in their domains of definition to be suitable to represent a biological situation.

2.1 Equilibrium solution and characteristic equation

In general, studies on influence of time delays on biological models consider one or more of five interesting cases: stability invariance, instability invariance, stability change, instability change, and instability switching of equilibria [3,10]. Studies on mathematical models of infectious diseases such as equation (2.1) considers two types of equilibria, viz, a disease-free equilibrium and an epidemic equilibrium. However, in our present study, as we are interested in the environment where the disease, i.e. the COVID-19 infection, persists under the influence of time delays, we consider only the existence of a disease equilibrium and establish conditions for stability of it, implying the prevalence of a disease environment. We assume that the endemic equilibrium solution of the system (2.1), denoted by (x^*, y^*, z^*), exists and is unique, recalling the conditions on parameters and functional relations in the study by Anand et al. [1], as time delays have no impact on the existence of equilibria. For simplicity, hereafter, we assume the growth function $f(x)$ as a constant, say $f(x) = k$, throughout the text.

In order to study the local stability of this endemic equilibrium solution, we first linearise the system (2.1) around the endemic equilibrium point (x^*, y^*, z^*). For simplicity, we will denote $x(t - \tau_1)$ as x_{τ_1} and $x(t - \tau_2)$ as x_{τ_2}. The linearised system with respect to the endemic equilibrium point is given as follows:

$$\begin{bmatrix} x'(t) \\ y'(t) \\ z'(t) \end{bmatrix} = \begin{bmatrix} H & A_1 & A_2 \\ 0 & B_1 & B_2 \\ 0 & C_1 & C_2 \end{bmatrix} \begin{bmatrix} x(t) \\ y(t) \\ z(t) \end{bmatrix} + \begin{bmatrix} 0 & 0 & 0 \\ \alpha D_1 & 0 & 0 \\ (1-\alpha)D_1 & 0 & 0 \end{bmatrix} \begin{bmatrix} x_{\tau_1} \\ 0 \\ 0 \end{bmatrix} + \begin{bmatrix} 0 & 0 & 0 \\ \beta D_2 & 0 & 0 \\ (1-\beta)D_2 & 0 & 0 \end{bmatrix} \begin{bmatrix} x_{\tau_2} \\ 0 \\ 0 \end{bmatrix}, \tag{2.2}$$

where $H = -d - af_1'(x)y - bf_2'(x)z$, $A_1 = p\alpha_1 - af_1(x)$, $A_2 = q\alpha_2 - bf_2(x)$, $B_1 = a_1af_1(x_{\tau_1}) - d_1 - \alpha_1$, $B_2 = b_1\beta f_2(x_{\tau_2})$, $C_1 = a_1(1-\alpha)f_1(x_{\tau_1})$, $C_2 = b_1(1-\beta)f_2(x_{\tau_2}) - d_2 - \alpha_2$, $D_1 = a_1f_1'(x_{\tau_1})y$, and $D_2 = b_1f_2'(x_{\tau_2})z$. Let us assume

$$S = \begin{bmatrix} H & A_1 & A_2 \\ 0 & B_1 & B_2 \\ 0 & C_1 & C_2 \end{bmatrix}, \quad T = \begin{bmatrix} 0 & 0 & 0 \\ \alpha D_1 & 0 & 0 \\ (1-\alpha)D_1 & 0 & 0 \end{bmatrix}, \quad U = \begin{bmatrix} 0 & 0 & 0 \\ \beta D_2 & 0 & 0 \\ (1-\beta)D_2 & 0 & 0 \end{bmatrix}.$$

Then, the characteristic equation corresponding to the endemic equilibrium point (x^*, y^*, z^*) is given as follows:

$$F(m) = \det(mI - S - T - U) = 0,$$

where I is the identity matrix. Hence, the characteristic equation is

$$F(m) = m^3 + l_1 m^2 + l_2 m + l_3 + l_4 e^{-m\tau_1} + l_5 e^{-m\tau_2} + l_6 m e^{-m\tau_1} + l_7 m e^{-m\tau_2}, \tag{2.3}$$

where $l_1 = -(H + B_1 + C_2)$, $l_2 = B_1 C_2 - B_2 C_1 + (B_1 + C_2)H$, $l_3 = -H(B_1 C_2 - B_2 C_1)$, $l_4 = \alpha A_1 C_2 D_1 - (1 - \alpha)A_1 B_2 D_1 - \alpha A_2 C_1 D_1 + (1 - \alpha)A_2 B_1 D_1$, $l_5 = \beta A_1 C_2 D_2 - (1 - \beta)A_1 B_2 D_2 - \beta A_2 C_1 D_2 + (1 - \beta)A_2 B_1 D_2$, $l_6 = -\alpha A_1 D_1 - (1 - \alpha)A_2 D_1$, and $l_7 = -\beta A_1 D_2 - (1 - \beta)A_2 D_2$.

We shall now proceed to find the stability of the endemic equilibrium point, which enables us to understand the importance of the delay parameters τ_1 and τ_2 and the role they are playing in ensuring the stability of the system in hand.

3 Local stability analysis

In this section, we study the local stability of the endemic equilibrium point (x^*, y^*, z^*) of the system (2.1). We will consider the following different cases:

 (i) $\tau_1 > 0$, $\tau_2 = 0$: Here, we consider that there is a latency or incubation period of the COVID-19 virus in the diabetic population; however, in the non-diabetic population, the symptoms arrive as soon as they are infected.

 (ii) $\tau_1 = 0$, $\tau_2 > 0$: This is the opposite of the above case. That is, there is no latency or incubation period of the COVID-19 virus in the diabetic population, but the non-diabetic population takes some time to show the symptoms.

(iii) $\tau_1 > 0$, $\tau_2 > 0$: This is the most realistic real-life scenario. Both the populations (diabetic and non-diabetic) are taking time to show the symptoms after getting infected by COVID-19.

Here, we will consider these cases and find the range of the time delays, for which the endemic equilibrium point will be locally stable.

3.1 Delay in incubation of diabetic population ($\tau_1 > 0$, $\tau_2 = 0$)

This is the case where there is no latency or incubation period of the infection in the non-diabetic population, but the diabetic population takes time $\tau_1 > 0$ to show first sign of symptoms.

The characteristic equation (2.3) in this case becomes

$$F(m, \tau_1) = m^3 + l_1 m^2 + (l_2 + l_7)m + l_3 + l_5 + (l_4 + l_6 m)e^{-m\tau_1}. \tag{3.1}$$

We rewrite the characteristic equation (3.1) as $F(m, \tau_1) = P(m) + Q(m)e^{-m\tau_1}$, where,

$$P(m) = m^3 + l_1 m^2 + (l_2 + l_7)m + l_3 + l_5 \quad \text{and} \quad Q(m) = l_4 + l_6 m. \tag{3.2}$$

We will denote the real and imaginary parts of the root m by $\Re(m)$ and $\Im(m)$, respectively. Let us consider the following result, which will help us estimate delays in such cases.

Lemma 3.1. *A system with characteristic equation $F(m, \tau_1) = P(m) + Q(m)e^{-m\tau_1}$ is asymptotically stable if and only if the following conditions are satisfied* [14,27]:
 (i) $F_1(m) = P(m) + Q(m) \neq 0$, $\Re(m) \geq 0$,
 (ii) $F_2(m) = P(m) - Q(m) \neq 0$, $\Re(m) = 0$, $m \neq 0$,
(iii) $F_3(m) = P(m) + \frac{1 - mR}{1 + mR}Q(m) \neq 0$, $\Re(m) = 0$, $m \neq 0$, $0 < R < \infty$,

where R denotes the pseudo-delay and is related to τ_1 as $\tau_1 = \frac{2}{v}(\tan^{-1}(vR) + k\pi)$, $\forall k \in \mathbb{Z}$.

The condition (*i*) in Lemma 3.1 ensures stability for $\tau_1 = 0$; hence, by continuity of solutions, this condition ensures stability even for sufficiently small delay $\tau_1 > 0$; (*ii*) confirms that no pure imaginary zeros exist in the limiting case; and condition (*iii*) establishes the absence of imaginary zeros. F_1, F_2, and F_3 are obtained by letting $e^{-m\tau_1} = 1, -1$, and $\frac{1-mR}{1+mR}$, respectively. Lemma 3.1 is a necessary and sufficient condition, and violation of any of the conditions (*i*), (*ii*), or (*iii*) reflects corresponding change in stability of characteristic equation $F(m, \tau_1) = P(m) + Q(m)e^{-m\tau_1}$. For more details on the applicability of this lemma, one may refer to [14].

Using Lemma 3.1, we will find the conditions for the preservation of stability in the system. We have, $F(m, \tau_1) = P(m) + Q(m)e^{-m\tau_1}$. Putting $e^{-m\tau_1} = 1$, we obtain

$$F_1(m) = P(m) + Q(m) = m^3 + l_1 m^2 + (l_2 + l_7)m + l_3 + l_5 + l_4 + l_6 m \neq 0 \tag{3.3}$$

for $\Re(m) \geq 0$.

Next, let $e^{-m\tau_1} = -1$, then

$$F_2(m) = P(m) - Q(m) = m^3 + l_1 m^2 + (l_2 - l_6 + l_7)m + l_3 + l_5 - l_4. \tag{3.4}$$

Let us now put, $m = iv$ in equation (3.4). Then,

$$F_2(iv) = -iv^3 - l_1 v^2 + iv(l_2 - l_6 + l_7) + l_3 - l_4 + l_5. \tag{3.5}$$

Clearly, $F_2(m) = 0$ if and only if $v^2 = l_2 - l_6 + l_7$ and $v^2 = \frac{l_3 - l_4 + l_5}{l_1}$. Hence, we can say that, $F_2(m) \neq 0$ for $\Re(m) = 0, m \neq 0$, if the following condition holds ensuring that no purely imaginary zeros exist in the limiting case:

$$(l_2 - l_6 + l_7)l_1 \neq l_3 - l_4 + l_5. \tag{3.6}$$

Finally, let $e^{-m\tau_1} = \frac{1-mR}{1+mR}$, for some $R > 0$. Then, $F_3(m)$ becomes

$$F_3(m) = P(m) + \frac{1-mR}{1+mR}Q(m).$$

Substituting $P(m)$ and $Q(m)$ in the above equation, we obtain

$$F_3(m) = \frac{m^4 R + m^3(1 + l_1 R) + m^2(l_1 + R(l_2 + l_7 - l_6))}{1 + mR}$$
$$+ \frac{m(l_2 + l_6 + l_7 + R(l_3 + l_5 - l_4)) + l_3 + l_4 + l_5}{1 + mR}. \tag{3.7}$$

Now, if we can show that $F_3(m) \neq 0$ for $\Re(m) = 0, m \neq 0, 0 < R < \infty$, then equation (3.1) has no pure imaginary zeros. In addition, $F_3(m) = 0$ only if numerator is equal to 0. Hence, we will assume that $l_3 + l_4 + l_5 \neq 0$, otherwise $m = 0$. Putting $m = iv$ in numerator of $F_3(m)$, we obtain

$$F_3(iv) = v^4 R - iv^3(1 + l_1 R) - v^2(l_1 + R(l_2 + l_7 - l_6))$$
$$+ iv(l_2 + l_6 + l_7 + R(l_3 + l_5 - l_4)) + l_3 + l_4 + l_5. \tag{3.8}$$

Separating real and imaginary parts, we obtain

$$\Re(F_3) = v^4 R - v^2(l_1 + R(l_2 + l_7 - l_6)) + l_3 + l_4 + l_5,$$
$$\Im(F_3) = -v^3(1 + l_1 R) + v(l_2 + l_6 + l_7 + R(l_3 + l_5 - l_4)).$$

From the $\Im(F_3)$ part, we have $v \neq 0$, hence $v^2 = \frac{l_2 + l_6 + l_7 + R(l_3 - l_4 + l_5)}{1 + l_1 R}$. Thus, no real v exists if $l_2 + l_6 + l_7 + R(l_3 - l_4 + l_5) < 0$ for any $R > 0$, establishing that there is no change in stability for any $\tau_1 \geq 0$. Next, using this value of v^2 and putting in $\Re(F_3)$, we obtain

$$M_1 R^3 + N_1 R^2 + P_1 R + Q_1 = 0, \tag{3.9}$$

where M_1, N_1, P_1, and Q_1 are given as follows:

(i) $M_1 = (l_3 - l_4 + l_5)^2 - l_1(l_3 - l_4 + l_5)(l_2 - l_6 + l_7)$,

(ii) $N_1 = 2(l_2 + l_6 + l_7)(l_3 - l_4 + l_5)$
   $+ l_1^2(l_3 + l_4 + l_5) + l_1 l_6^2 - l_1(l_2 + l_7)^2 - (l_2 - l_6 + l_7)(l_3 - l_4 + l_5) - l_1^2(l_3 - l_4 + l_5)$,

(iii) $P_1 = (l_2 + l_6 + l_7)^2 + 2l_1(l_3 + l_4 + l_5) - (l_2 + l_7)^2 + l_6{}^2 - l_1(l_3 - l_4 + l_5) - l_1{}^2(l_2 + l_7 + l_6)$,

(iv) $Q_1 = l_3 + l_4 + l_5 - l_1(l_2 + l_6 + l_7)$.

Hence, we have the following theorem.

Theorem 3.1. *Assume the endemic equilibrium solution of equation* (2.1) *is locally stable for* $\tau_1 = \tau_2 = 0$. *Then, for any length of delay* $\tau_1 > 0$, $\tau_2 = 0$, *the endemic equilibrium solution is locally stable if the following conditions hold*:

(i) $(l_2 - l_6 + l_7)l_1 \neq l_3 - l_4 + l_5$,

(ii) $M_1, N_1, P_1, Q_1 > 0$,

(iii) $N_1 P_1 > M_1 Q_1$.

A change of stability occurs at $\tau_1 = \tau_1{}^+ > 0$ *if any of the coefficient* M_1, N_1, P_1, *or* Q_1 *is negative. Here,* $\tau_1{}^+ = \frac{2}{v^+} \tan^{-1}(v^+ R^+)$, *where*

$$v^+ = \sqrt{\frac{l_2 + l_6 + l_7 + R(l_3 - l_4 + l_5)}{1 + l_1 R}}$$

and R^+ *is solution of equation* (3.9).

3.2 Delay in incubation of non-diabetic population ($\tau_1 = 0$, $\tau_2 > 0$)

This case corresponds to the scenario where there is no latency or incubation period of the infection in the diabetic population, but the non-diabetic population takes time $\tau_2 > 0$ to show first sign of symptoms.

We have $\tau_1 = 0$, $\tau_2 > 0$. Then, equation (2.3) becomes

$$F(m, \tau_2) = m^3 + l_1 m^2 + (l_2 + l_6)m + l_3 + l_4 + e^{-m\tau_2}(l_5 + l_7 m). \tag{3.10}$$

Let us write the characteristic equation (3.10) as $F(m, \tau_2) = P(m) + Q(m)e^{-m\tau_2}$, where

$$P(m) = m^3 + l_1 m^2 + (l_2 + l_6)m + l_3 + l_4, \quad Q(m) = l_5 + l_7 m. \tag{3.11}$$

Similar as the above case, we have $F(m, \tau_2) = P(m) + Q(m)e^{-m\tau_2}$, and we will use Lemma 3.1 to study the stability of this system. Putting $e^{-m\tau_2} = 1$, we obtain

$$F_1(m) = P(m) + Q(m) = m^3 + l_1 m^2 + (l_2 + l_6)m + l_3 + l_4 + l_5 + l_7 m \neq 0 \tag{3.12}$$

for $\Re(m) \geq 0$, ensuring stability for $\tau_2 = 0$.

Next, let $e^{-m\tau_2} = -1$, then

$$F_2(m) = P(m) - Q(m) = m^3 + l_1 m^2 + (l_2 + l_6 - l_7)m + l_3 + l_4 - l_5. \tag{3.13}$$

Let us now put, $m = iv$. Then,

$$F_2(iv) = -iv^3 - l_1 v^2 + iv(l_2 + l_6 - l_7) + l_3 + l_4 - l_5. \tag{3.14}$$

Clearly, $F_2(m) = 0$ if $v^2 = l_2 + l_6 - l_7$ and $v^2 = \frac{l_3 + l_4 - l_5}{l_1}$. Hence, we can say that, $F_2(m) \neq 0$, and there exists no pure imaginary zeros in limiting case if

$$l_1(l_2 + l_6 - l_7) \neq l_3 + l_4 - l_5. \tag{3.15}$$

Finally, let $e^{-m\tau_2} = \frac{1 - mR}{1 + mR}$ for some $R > 0$. Then, $F_3(m)$ becomes

$$F_3(m) = P(m) + \frac{1 - mR}{1 + mR}Q(m).$$

Substituting $P(m)$ and $Q(m)$ in the above equation, we obtain

$$F_3(m) = \frac{m^4 R + m^3(1 + l_1 R) + m^2(l_1 + R(l_2 + l_6 - l_7))}{1 + mR}$$
$$+ \frac{m(l_2 + l_6 + l_7 + R(l_3 + l_4 - l_5)) + l_3 + l_4 + l_5}{1 + mR}. \tag{3.16}$$

Therefore, $F_3(m) = 0$ only if numerator is equal to 0. Hence, $l_3 + l_4 + l_5 \neq 0$; otherwise, $m = 0$. For pure imaginary zeros, putting $m = iv$ in numerator of $F_3(m)$, we obtain

$$F_3(iv) = v^4 R - iv^3(1 + l_1 R) - v^2(l_1 + R(l_2 + l_6 - l_7))$$
$$+ iv(l_2 + l_6 + l_7 + R(l_3 + l_4 - l_5)) + l_3 + l_4 + l_5. \tag{3.17}$$

Separating real and imaginary parts, we obtain

$$\Re(F_3) = v^4 R - v^2(l_1 + R(l_2 + l_6 - l_7)) + l_3 + l_4 + l_5,$$
$$\Im(F_3) = -v^3(1 + l_1 R) + v(l_2 + l_6 + l_7 + R(l_3 + l_4 - l_5)).$$

From the $\Im(F_3)$ part, we have $v \neq 0$, hence $v^2 = \frac{l_2 + l_6 + l_7 + R(l_3 + l_4 - l_5)}{1 + l_1 R}$. Thus, no real v exists if $l_2 + l_6 + l_7 + R(l_3 + l_4 - l_5) < 0$ for $R > 0$, establishing that stability is preserved for any length of delay $\tau_2 > 0$. Next, using this value of v^2 and putting in $\Re(F_3)$, we obtain

$$M_2 R^3 + N_2 R^2 + P_2 R + Q_2 = 0, \tag{3.18}$$

where

(i) $M_2 = (l_3 + l_4 - l_5)^2 - l_1(l_3 + l_4 - l_5)(l_2 + l_6 - l_7)$,

(ii) $N_2 = 2(l_2 + l_6 + l_7)(l_3 + l_4 - l_5)$
  $+ l_1 l_7^2 - l_1(l_2 + l_6)^2 + l_1^2(l_3 + l_4 + l_5) - (l_2 + l_6 - l_7)(l_3 + l_4 - l_5) - l_1^2(l_3 + l_4 - l_5)$,

(iii) $P_2 = (l_2 + l_6 + l_7)^2 + 2l_1(l_3 + l_4 + l_5) - (l_2 + l_6)^2 + l_7^2 - l_1(l_3 + l_4 - l_5) - l_1^2(l_2 + l_7 + l_6)$,

(iv) $Q_2 = l_3 + l_4 + l_5 - l_1(l_2 + l_6 + l_7)$.

We have the following theorem.

Theorem 3.2. *Assume the endemic equilibrium solution to equation* (2.1) *is locally stable for $\tau_1 = \tau_2 = 0$. Then, for any length of delay $\tau_1 = 0$, $\tau_2 > 0$, the endemic equilibrium solution is locally stable if the following conditions hold:*

(i) $l_1(l_2 + l_6 - l_7) \neq l_3 + l_4 - l_5$,

(ii) $M_2, N_2, P_2, Q_2 \geq 0$,

(iii) $N_2 P_2 > M_2 Q_2$.

A change of stability occurs at $\tau_2 = \tau_2^+ > 0$ if any of the coefficient M_2, N_2, P_2, or Q_2 is negative. Here, $\tau_2^+ = \frac{2}{v^+} \tan^{-1}(v^+ R^+)$, where

$$v^+ = \sqrt{\frac{l_2 + l_6 + l_7 + R(l_3 + l_4 - l_5)}{1 + l_1 R}}$$

and R^+ is solution to equation (3.18).

3.3 Delays in incubation of both diabetic and non-diabetic populations ($\tau_1, \tau_2 > 0$)

This is the most important and relevant scenario, where the incubation periods τ_1 and τ_2 of both the populations are greater than zero.

Letting $m = \mu + iv$ in equation (2.3), then μ and v are real solutions of

$$\Re(F(\mu, \nu)) = \mu^3 - 3\mu\nu^2 + l_1(\mu^2 - \nu^2) + l_2\mu + l_3 + l_4 \cos(\nu\tau_1)e^{-\tau_1\mu} + l_5 \cos(\nu\tau_2)e^{-\tau_2\mu}$$
$$+ l_6(\mu \cos(\nu\tau_1) + \nu \sin(\nu\tau_1))e^{-\tau_1\mu} + l_7(\mu \cos(\nu\tau_2) + \nu \sin(\nu\tau_2))e^{-\tau_2\mu},$$
$$\Im(F(\mu, \nu)) = 3\mu^2\nu - \nu^3 + 2l_1\mu\nu + l_2\nu - l_4 \sin(\nu\tau_1)e^{-\tau_1\mu} - l_5 \sin(\nu\tau_2)e^{-\tau_2\mu}$$
$$+ l_6(\nu \cos(\nu\tau_1) - \mu \sin(\nu\tau_1))e^{-\tau_1\mu} + l_7(\nu \cos(\nu\tau_2) - \mu \sin(\nu\tau_2))e^{-\tau_2\mu}.$$

To find the condition for change of stability, we substitute $\mu = 0$ in the above equations to obtain

$$\Re(F(i\nu)) = -l_1\nu^2 + l_3 + l_4 \cos(\nu\tau_1) + l_5 \cos(\nu\tau_2) + l_6\nu \sin(\nu\tau_1) + l_7\nu \sin(\nu\tau_2), \tag{3.19}$$

$$\Im(F(i\nu)) = -\nu^3 + l_2\nu - l_4 \sin(\nu\tau_1) - l_5 \sin(\nu\tau_2) + l_6\nu \cos(\nu\tau_1) + l_7\nu \cos(\nu\tau_2). \tag{3.20}$$

For the preservation of the stability of the delay system, we use the following conditions of the Nyquist criteria $\Im(F(i\nu_0)) > 0$ and $\Re(F(i\nu_0)) = 0$, where ν_0 is the smallest positive root of $\Re(F(i\nu_0)) = 0$. For more details, we refer to [7,9].

Let $\nu = \nu_0$ be the smallest positive root of $\Re(F(i\nu)) = 0$. We write $\Re(F(i\nu)) = 0$ as

$$l_1\nu^2 - l_3 = l_4 \cos(\nu\tau_1) + l_5 \cos(\nu\tau_2) + l_6\nu \sin(\nu\tau_1) + l_7\nu \sin(\nu\tau_2). \tag{3.21}$$

After replacing sin and cos by their maximum values, we rewrite the above equation (3.21) as follows:

$$l_1\nu^2 - l_3 < |l_4| + |l_5| + |\nu||l_6| + |\nu||l_7|.$$

Let us consider the equation

$$l_1\nu_0{}^2 - \nu_0(|l_6| + |l_7|) - l_3 - |l_4| - |l_5| = 0. \tag{3.22}$$

The quadratic equation (3.22) has two roots, and let ν_+ be the bigger root, which is given as follows:

$$\nu_+ = \frac{|l_6| + |l_7| + \sqrt{|l_6|^2 + |l_7|^2 + 2|l_6||l_7| + 4l_1(l_3 + |l_4| + |l_5|)}}{2l_1}. \tag{3.23}$$

We now use $\Im(F(i\nu_0)) > 0$ and obtain

$$-\nu^3 + l_2\nu + l_6\nu \cos(\nu\tau_1) + l_7\nu \cos(\nu\tau_2) > l_4 \sin(\nu\tau_1) + l_5 \sin(\nu\tau_2). \tag{3.24}$$

Let, $\phi = -\nu^3 + l_2\nu + l_6\nu \cos(\nu\tau_1) + l_7\nu \cos(\nu\tau_2)$ and $\psi = l_4 \sin(\nu\tau_1) + l_5 \sin(\nu\tau_2)$. Then, clearly $\phi > \psi$.

We now need to find the range of the delay for which the system will be stable. We observe that $\psi < (|l_4| + |l_5|)\nu_+(\tau_1 + \tau_2)$. Hence,

$$\frac{\psi}{(\tau_1 + \tau_2)\nu_+} \leq |l_4| + |l_5|.$$

In addition,

$$\frac{\phi}{\nu_+} \leq \nu_+{}^2 + |l_2| + |l_6|\cos(\nu_+\tau_1) + |l_7|\cos(\nu_+\tau_2) < \nu_+{}^2 + |l_2| + |l_6| + |l_7|.$$

Therefore,

$$\frac{\phi}{(\tau_1 + \tau_2)\nu_+} \leq \frac{\nu_+{}^2 + |l_2| + |l_6| + |l_7|}{\tau_1 + \tau_2}.$$

Hence, we can write

$$|l_4| + |l_5| < \frac{\nu_+{}^2 + |l_2| + |l_6| + |l_7|}{\tau_1 + \tau_2}.$$

Thus, we obtain

$$(\tau_1 + \tau_2) < \frac{\nu_+{}^2 + |l_2| + |l_6| + |l_7|}{|l_4| + |l_5|}. \tag{3.25}$$

Hence, we can formulate the following theorem.

Theorem 3.3. *Assume that the endemic equilibrium point of equation* (2.1) *is locally stable for* $\tau_1 = \tau_2 = 0$. *Then, the stability of the endemic equilibrium point is preserved for* $\tau_1, \tau_2 > 0$ *if*

$$(\tau_1 + \tau_2) < \frac{v_+^2 + |l_2| + |l_6| + |l_7|}{|l_4| + |l_5|}.$$

Remark. Note that condition (i) of Lemma 3.1 discusses the case of delay-free system $\tau_1 = \tau_2 = 0$. Thus, from equation (3.3), we have

$$F(m) = m^3 + l_1 m^2 + (l_2 + l_6 + l_7)m + l_3 + l_4 + l_5. \tag{3.26}$$

Hence, if the parameters of the system satisfy the conditions

$$l_1 > 0, l_2 + l_6 + l_7 > 0, l_3 + l_4 + l_5 > 0, l_1(l_2 + l_6 + l_7) > l_3 + l_4 + l_5,$$

then equation (3.26) will have all the roots with negative real parts. Therefore, the system (2.1) is asymptotically stable for $\tau_1 = \tau_2 = 0$ if the above conditions hold true. We observe that our results are matching with those of Theorem 3.3 of [1].

We now proceed to find the global stability of the endemic equilibrium point of equation (2.1).

4 Global stability analysis

Global stability is an important study in disease dynamics, which specifies the stability of the equilibrium in the broader sense – whether the equilibrium point is always stable irrespective of the changes in the initial conditions. In this section, we will deal with the global stability aspect of the endemic equilibrium point. We make the following assumptions on the conversion functions f_1 and f_2 before we establish our results.

$$0 \leq \mathcal{M}_1 \leq f_1(x) \leq \mathcal{N}_1, \qquad 0 \leq \mathcal{M}_2 \leq f_2(x) \leq \mathcal{N}_2, \tag{4.1}$$

for all x. These assumptions are realistic in view of examples of conversion functions that are commonly used in such biological scenarios mentioned in Section 2.

4.1 Global stability analysis for endemic equilibrium point

Let (x^*, y^*, z^*) be the endemic equilibrium point. Then, they satisfy the following equations:

$$0 = k - dx^* - af_1(x^*)y^* - bf_2(x^*)z^* + pa_1y^* + qa_2z^*, \tag{4.2}$$

$$0 = a_1 af_1(x^*)y^* + b_1\beta f_2(x^*)z^* - (d_1 + a_1)y^*, \tag{4.3}$$

$$0 = a_1(1 - a)f_1(x^*)y^* + b_1(1 - \beta)f_2(x^*)z^* - (d_2 + a_2)z^*. \tag{4.4}$$

Subtracting equations (4.2)–(4.4) from equation (2.1) and rearranging, we obtain

$$(x - x^*)' = -d(x - x^*) - af_1(x)(y - y^*) - ay^*(f_1(x) - f_1(x^*))$$
$$- bf_2(x)(z - z^*) - bz^*(f_2(x) - f_2(x^*)) + pa_1(y - y^*) + qa_2(z - z^*), \tag{4.5}$$

$$(y - y^*)' = a_1 af_1(x_{\tau_1})(y - y^*) + a_1 ay^*(f_1(x_{\tau_1}) - f_1(x^*)) + b_1\beta f_2(x_{\tau_2})(z - z^*)$$
$$+ b_1\beta z^*(f_2(x_{\tau_2}) - f_2(x^*)) - d_1(y - y^*) - a_1(y - y^*), \tag{4.6}$$

$$(z - z^*)' = a_1(1 - a)f_1(x_{\tau_1})(y - y^*) + a_1(1 - a)y^*(f_1(x_{\tau_1}) - f_1(x^*)) + b_1(1 - \beta)f_2(x_{\tau_2})(z - z^*)$$
$$+ b_1(1 - \beta)z^*(f_2(x_{\tau_2}) - f_2(x^*)) - d_2(z - z^*) - a_2(z - z^*). \tag{4.7}$$

Let us assume that there exist positive real constants S_1 and S_2 such that

$$|f_1(x) - f_1(x^*)| \le S_1|x - x^*|, \quad |f_2(x) - f_2(x^*)| \le S_2|x - x^*|, \tag{4.8}$$

where $x \ne x^*$. We are now in a position to establish global stability of the endemic equilibrium. We employ a Lyapunov-Krasovskii-type functional to cancel out the delay terms and manipulate the delay-free terms using inequality analysis [17]. We note that the functional employed in [27] is also applicable here. Now we have the following theorem.

Theorem 4.1. *The endemic equilibrium point (x^*, y^*, z^*) of the system* (2.1)*is globally asymptotically stable if the following conditions hold*:

(i) $d - (a - a_1)y^*S_1 - (b - b_1)z^*S_2 > 0$,

(ii) $d_1 + (1 - p)\alpha_1 + a\mathcal{M}_1 - a_1\mathcal{N}_1 > 0$, *and*

(iii) $d_2 + (1 - q)\alpha_2 + b\mathcal{M}_2 - b_1\mathcal{N}_2 > 0$,

where $\mathcal{M}_1$, $\mathcal{N}_1$, and $\mathcal{M}_2$, $\mathcal{N}_2$ are positive real constants defined above.

Proof. We consider the functional

$$V(t) \equiv V(x(t), y(t), z(t)) = |x - x^*| + |y - y^*| + |z - z^*| + a_1 y^* \int_{t-\tau_1}^{t} |f_1(x(u)) - f_1(x^*)| \mathrm{d}u \tag{4.9}$$

$$+ b_1 z^* \int_{t-\tau_2}^{t} |f_2(x(u)) - f_2(x^*)| \mathrm{d}u.$$

Clearly, $V(x^*, y^*, z^*) = 0$ and $V(t) \ge 0$. The upper Dini derivative of V along the solutions of the system (2.1) is given as follows:

$$\begin{aligned}
D^+V \le &-d|x - x^*| - af_1(x)|y - y^*| - ay^*|f_1(x) - f_1(x^*)| - bf_2(x)|z - z^*| \\
&- bz^*|f_2(x) - f_2(x^*)| + p\alpha_1|y - y^*| + q\alpha_2|z - z^*| + a_1 af_1(x_{\tau_1})|y - y^*| - d_1|y - y^*| \\
&+ a_1 ay^*|f_1(x_{\tau_1}) - f_1(x^*)| + b_1\beta f_2(x_{\tau_2})|z - z^*| + b_1\beta z^*|f_2(x_{\tau_2}) - f_2(x^*)| - \alpha_1|y - y^*| \\
&+ a_1(1 - \alpha)f_1(x_{\tau_1})|y - y^*| + a_1(1 - \alpha)y^*|f_1(x_{\tau_1}) - f_1(x^*)| + b_1(1 - \beta)f_2(x_{\tau_2})|z - z^*| \\
&+ b_1(1 - \beta)z^*|f_2(x_{\tau_2}) - f_2(x^*)| - d_2|z - z^*| - \alpha_2|z - z^*| + a_1 y^* \int_{t-\tau_1}^{t} |f_1(x(u)) - f_1(x^*)| \mathrm{d}u \\
&+ b_1 z^* \int_{t-\tau_2}^{t} |f_2(x(u)) - f_2(x^*)| \mathrm{d}u.
\end{aligned}$$

After simplifying, we obtain

$$\begin{aligned}
D^+V \le &-d|x - x^*| - (d_1 + (1 - p)\alpha_1)|y - y^*| - (d_2 + (1 - q)\alpha_2)|z - z^*| - |y - y^*||af_1(x) - a_1 f_1(x_{\tau_1})| \\
&- |z - z^*||bf_2(x) - b_1 f_2(x_{\tau_2})| - (a - a_1)y^*|f_1(x) - f_1(x^*)| - (b - b_1)z^*|f_2(x) - f_2(x^*)|.
\end{aligned} \tag{4.10}$$

We rewrite the above equation (4.10) by using the bounds (4.1) and (4.8), and we arrive at

$$\begin{aligned}
D^+V < &-|x - x^*|(d - (a - a_1)y^*S_1 - (b - b_1)z^*S_2) - (d_1 + (1 - p)\alpha_1 + af_1(x) - a_1\mathcal{N}_1)|y - y^*| \\
&- (d_2 + (1 - q)\alpha_2 + bf_2(x) - b_1\mathcal{N}_2)|z - z^*| \\
\le &-(d - (a - a_1)y^*S_1 - (b - b_1)z^*S_2)|x - x^*| - (d_1 + (1 - p)\alpha_1 + a\mathcal{M}_1 - a_1\mathcal{N}_1)|y - y^*| \\
&- (d_2 + (1 - q)\alpha_2 + b\mathcal{M}_2 - b_1\mathcal{N}_2)|z - z^*| < 0
\end{aligned}$$

by assumptions (i)–(iii). Thus, $V(t)$ is negative definite. Furthermore, by definition $V(t) \ge 0$ and $V(t) = V(x, y, z) = 0$ if and only if $x = x^*, y = y^*, z = z^*$. Thus, $V(t)$ is a suitable Lyapunov functional. This completes the proof.　　□

We shall now present some illustrative examples in order to verify the results.

5 Numerical experiments

In this section, we perform some numerical experiments to validate our theoretical results using MATLAB software dde23. Since, we could not obtain a single source of data to reflect all parameters, we have assumed the parameters to illustrate the results. We perform simulations for various lengths of delays in all three cases, i.e. (i) $\tau_1 = \tau_2 = 0$, (ii) $\tau_1 > 0$, $\tau_2 = 0$, (iii) $\tau_1 = 0$, $\tau_2 > 0$, and (iv) $\tau_1 > 0$, $\tau_2 > 0$. The motive of this study is to find the incubation time of the COVID-19 virus in the diabetic and non-diabetic population, depending on the different parameters. We will assume the units of the parameters to be as per day.

Example 1. We consider the system (2.1) with high exposure rates a and b and low conversion rates a_1 and b_1. We also take the treatment parameters α_1 and α_2 to be nearly equal to the conversion rates, and the mortality rates (d, d_1, d_2) are taken as low values. Let $f_1(x) = f_2(x) = \frac{x}{1+x}$ and $\alpha = \beta$. Let the parameter values be $k = 300$, $d = 0.0001$, $a = 2$, $b = 3$, $p = 0.5$, $q = 0.2$, $\alpha_1 = 0.7$, $\alpha_2 = 0.5$, $\alpha = 0.5$, $a_1 = 0.75$, $b_1 = 0.5$, $d_1 = 0.01$, and $d_2 = 0.008$. The initial populations are $x(t) = 100$, $y(t) = 20$, $z(t) = 80$, $t \in [-\tau, 0]$, and $\tau = \max\{\tau_1, \tau_2\}$. The endemic equilibrium point of the system (2.1) is given by $(x^*, y^*, z^*) = (49, 54, 75)$.

Delay free. Let $\tau_1 = \tau_2 = 0$. Then, we see that all the conditions for delay-free system are satisfied. The solution profile of the delay-free case is given in Figure 2.

Case 1 ($\tau_1 > 0$, $\tau_2 = 0$). We calculate $M_1 = 0.00009$, $N_1 = 0.016$, $P_1 = -0.0046$, and $Q_1 = -0.066$ from Theorem 3.1. We see that there is one sign change in the equation $M_1 R^3 + N_1 R^2 + P_1 R + Q_1 = 0$, and hence from Routh-Hurwitz criteria, there exists one root R with positive real part, which is coming to be $R = 2.17706$. With this value of R, we obtain $v^+ = 0.236$ and $\tau_1^+ = 4.022$ from Theorem 3.1. Hence, theoretically, the system will be stable till $\tau_1^+ \leq 4.022$ for $\tau_2 = 0$ and will be unstable when $\tau_1^+ > 4.022$. Numerically, we can see from Figure 3, the solutions are approaching the equilibrium solution (x^*, y^*, z^*) for $\tau_1 = 4$, whereas for $\tau_1 = 4.2$, the solutions does not converge. Hence, stability change is clearly evident as per theory.

Case 2 ($\tau_1 = 0$, $\tau_2 > 0$). Here, $M_2 = -0.00009$, $N_2 = 0.014$, $P_2 = -0.0075$, and $Q_2 = -0.066$ from Theorem 3.2. Similar to the above case, we see that there are two sign changes in $M_2 R^3 + N_2 R^2 + P_2 R + Q_2 = 0$, and hence there exists two R with positive real parts. The positive roots are $R = 2.4528$ and $R = 155.58$. With $R = 155.58$, we obtain $\tau_2^+ = 50.4$. This high value of delay τ_2 may represent the case where the non-diabetic population is a carrier (strong immunity and/or does not show symptoms easily) but not identified as infected for a long time. Since, we are more interested in finding the incubation period after which the population will show symptom, we will not proceed with this case. With $R = 2.4528$, we obtain $v^+ = 0.2328$ and $\tau_2^+ = 4.4574$ from Theorem 3.2.
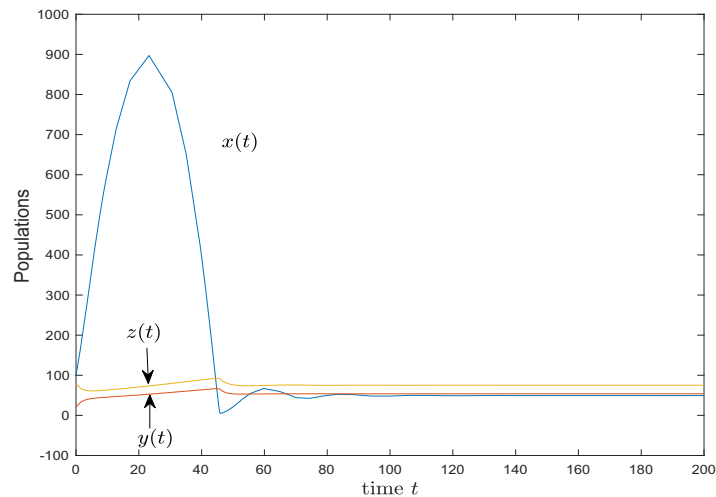

Figure 2: Solution profile for $\tau_1 = \tau_2 = 0$ of Example 1.

Hence, the system is stable for $\tau_2^+ \leq 4.4574$ when $\tau_1 = 0$. We see that numerically, from Figure 4, a change in τ_2 from 4.45 to 4.7 changes the stability of the system. Hence, our theoretical results are validated.

Case 3 ($\tau_1, \tau_2 > 0$). From Theorem 3.3, we find $\tau_1 + \tau_2 < 5.38$. Hence, the system should be stable till $\tau_1 + \tau_2 < 5.38$ and unstable when $\tau_1 + \tau_2 \geq 5.38$. From Figure 5, we see that the system is stable till $\tau_1 + \tau_2 \leq 3.6$.

Discussion. From our chosen set of parameter values, we see that the exposure rates a and b are much higher than the conversion rates a_1 and b_1, respectively. We took the treatment parameters α_1 and α_2 nearly equal to the conversion rates and the death rates are comparatively small. With these parameter values, we see that the system is becoming stable after long time, and if the delays or incubation time is crossing their threshold value, then the system starts oscillation. The delays or incubation periods estimated in this Example 1 are close to the real-life scenario [36]. We also note from the Figures 3–5 that the oscillation due to the delays are only in the x, i.e. the susceptible population, and there is no oscillation in the y and z populations. This is due to the fact that we have introduced the delay parameters only in the susceptible population and none in the infected diabetic and non-diabetic populations. As we are increasing the delay range, oscillations with higher amplitude are observed in the x population – a chaotic situation continues. In addition, the condition of global stability in Theorem 4.1 is not satisfied, and hence, the system is not globally stable around the equilibrium point $(x^*, y^*, z^*) = (49, 54, 75)$. That is, a small change in the initial conditions might give rise to instability around the equilibrium point $(x^*, y^*, z^*) = (49, 54, 75)$.

Example 2. In this example, we alter the conversion parameters (i.e. reduce a_1 and increase b_1) while increasing the proportions of recovered turning susceptible diabetic and non-diabetic populations (p and q). We let $f_1(x) = f_2(x) = \frac{x}{1+x}$ and $\alpha = \beta = 0.5$, $k = 300$, $d = 0.0001$, $a = 2$, $b = 3$, $p = 0.7$, $q = 0.3$, $\alpha_1 = 0.7$, $\alpha_2 = 0.5$, $a_1 = 0.6$, $b_1 = 0.6$, $d_1 = 0.01$, and $d_2 = 0.008$. The initial populations are $x(t) = 100$, $y(t) = 20$, $z(t) = 80$, $t \in [-\tau, 0]$, and $\tau = \max\{\tau_1, \tau_2\}$. The endemic equilibrium point is given by $(x^*, y^*, z^*) = (76, 55, 77)$.

Delay free. Let $\tau_1 = \tau_2 = 0$. Then, all the conditions for delay-free system are satisfied. The solution profile of the delay-free case is given in Figure 6.

Case 1 ($\tau_1 > 0, \tau_2 = 0$). We calculate $M_1 = -0.000075$, $N_1 = 0.0056$, $P_1 = -0.0056$, and $Q_1 = -0.0257$ from Theorem 3.1. We see that there are two sign changes in the equation $M_1 R^3 + N_1 R^2 + P_1 R + Q_1 = 0$, and hence, from Routh-Hurwitz criteria, there exists two roots R with positive real parts. The roots are $R = 2.7666$ and $R = 73.58$. With $R = 73.58$, we obtain very high values of τ_1; hence, as discussed in Case 2 of the previous example, we will not proceed with this scenario. With $R = 2.7666$, we obtain $v^+ = 0.16$ and $\tau_1^+ = 5.2135$ from Theorem 3.1. Hence, the system will be stable till $\tau_1^+ \leq 5.2135$ given $\tau_2 = 0$ and will be unstable when $\tau_1^+ > 5.2135$. Numerically, we see from Figure 7 that a change in τ_1 from 5 to 5.5 changes the stability of the system.

Case 2 ($\tau_1 = 0, \tau_2 > 0$). Here, $M_2 = 0.0000738$, $N_2 = 0.0083$, $P_2 = -0.00087$, and $Q_2 = -0.025$ from Theorem 3.2. Similar to the above example, we see that there is one sign change in the coefficients of
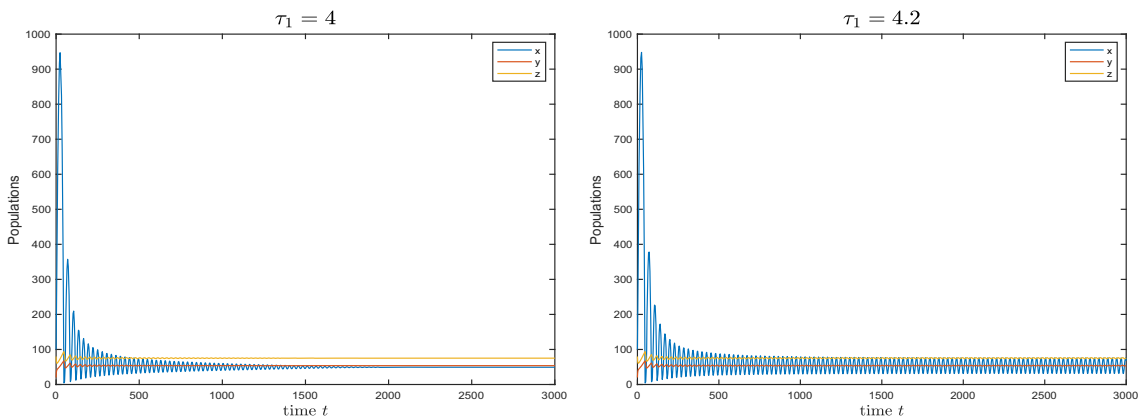

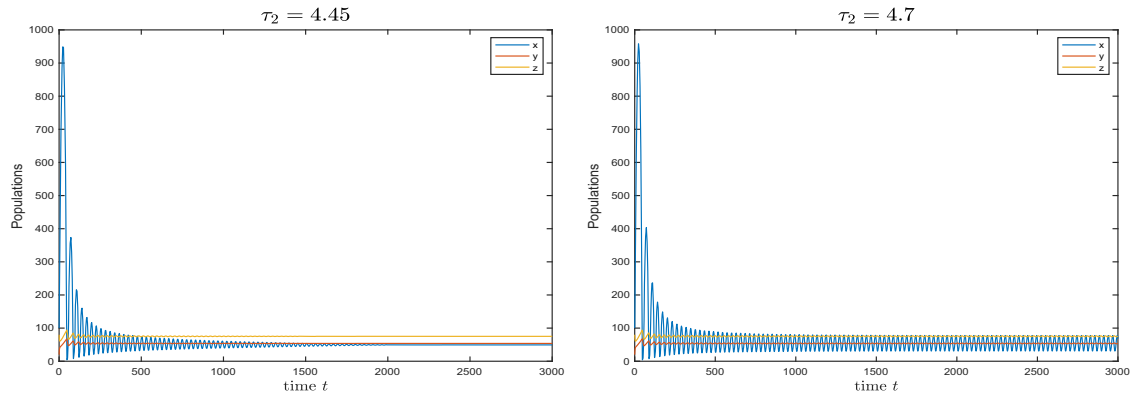**Figure 3:** Solution profiles for $\tau_1 > 0$, $\tau_2 = 0$.

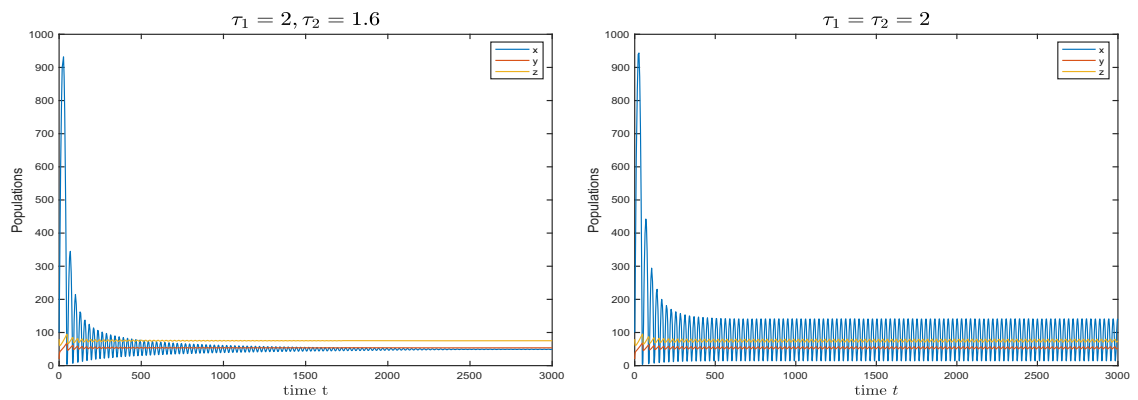**Figure 4:** Solution profiles for $\tau_1 = 0$, $\tau_2 > 0$.

Figure 5: Solution Profiles for τ_1, $\tau_2 > 0$.

$M_2R^3 + N_2R^2 + P_2R + Q_2 = 0$, and hence there exists one R with positive real part, which is $R = 1.7984$. With this R, we obtain $v^+ = 0.166$ and $\tau_2^+ = 3.5$ from Theorem 3.2. Hence, the system is stable for $\tau_2^+ \leq 3.5$ given $\tau_1 = 0$. From Figure 8, we observe that a change in τ_2 from 3.3 to 3.6 changes the stability of the system.

Case 3 (τ_1, $\tau_2 > 0$). From Theorem 3.3, we obtain $\tau_1 + \tau_2 < 5.413$. Hence, the system is stable till $\tau_1 + \tau_2 < 5.413$ and should be unstable for $\tau_1 + \tau_2 \geq 5.413$. From Figure 9, we see that the system is stable till $\tau_1 + \tau_2 \leq 3.7$.
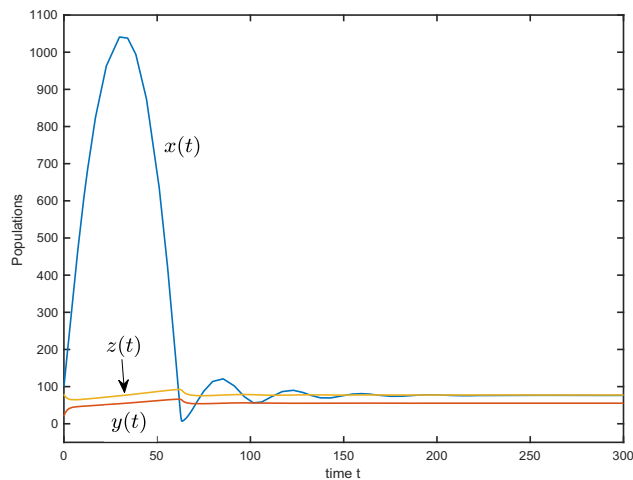

Figure 6: Solution profile for $\tau_1 = \tau_2 = 0$ of Example 2.

Discussion. In this example, we changed the conversion parameters slightly, i.e. reduced a_1 (conversion rate corresponding to the diabetic population) and increased b_1 (conversion rate corresponding to the non-diabetic population). Compared to Example 1, there have been changes in the delays (with τ_1 increasing and τ_2 slightly decreasing). These changes indicate that more non-diabetic individuals exposed to COVID-19 are transitioning into the infected population, implying a weaker immune response and a shorter incubation period (τ_2) compared to Example 1. On the other hand, the diabetic population exposed to the COVID-19 virus shows a lower rate of transition into the infected population compared to Example 1, suggesting better immunity due to medication. Consequently, the diabetic population has a longer incubation period compared to their non-diabetic counterparts. Similar to Example 1, we see from the Figures 7–9 that the oscillations are only in x, and none in y and z, and oscillations with larger amplitude are observed in the x population as we increase the delay values leading to a chaotic situation. The explanation of this phenomena is given in the discussion of Example 1. In addition, in this example, the condition of global stability in Theorem 4.1 is not satisfied, and hence, the system is not globally stable around the equilibrium point $(x^*, y^*, z^*) = (76, 55, 77)$.

Next, let us consider an example where the endemic equilibrium point (x^*, y^*, z^*) is globally asymptotically stable.

Example 3. In this example, we take the parameter values in the system (2.1) as $k = 300$, $d = 0.8$, $a = 1.2534$, $b = 2.1431$, $p = 0.5$, $q = 0.7$, $\alpha_1 = 5$, $\alpha_2 = 1$, $\alpha = 0.5$, $a_1 = 1.253$, $b_1 = 2.142$, $d_1 = 0.5$, $d_2 = 0.15$, $f_1(x) = f_2(x) = \frac{x}{1+x}$, and $\alpha = \beta$.

The endemic equilibrium point is given by $(x^*, y^*, z^*) = (22, 55, 262)$. We have chosen the parameters in such a way that the global stability of the endemic equilibrium point $(x^*, y^*, z^*) = (22, 55, 262)$ is satisfied, i.e. whenever the exposure (a, b) and conversion (a_1, b_1) rates are nearly equal, the treatment rates (α_1, α_2) are high compared to the mortality rates (d_1, d_2). We see that all the conditions of Theorem 4.1 are satisfied, and hence, our system is globally asymptotically stable.

We can see from Figure 10 that the stability of the delay-free system is independent of the initial populations, implying global stability.

Next, let us consider the system where both the delays exist, i.e. $\tau_1, \tau_2 > 0$. From Theorem 3.3, we obtain $\tau_1 + \tau_2 < 2.99$. Hence, the system is stable till $\tau_1 + \tau_2 < 2.99$. Below, we have given the following plots in Figure 11 for different initial populations for $\tau_1, \tau_2 > 0$.

Discussion. From Figures 10 and 11, we see that system behaves similarly irrespective of the presence of delays and change in initial conditions. We observe that for the case where $\tau_1, \tau_2 > 0$, the system is globally stable whenever $\tau_1 + \tau_2 < 2.99$.

Remark. From Examples 1 and 2, we observe how the parameters play an important role in influencing the time delays (incubation periods, in our case) of the system. In Example 1, our conversion rates from
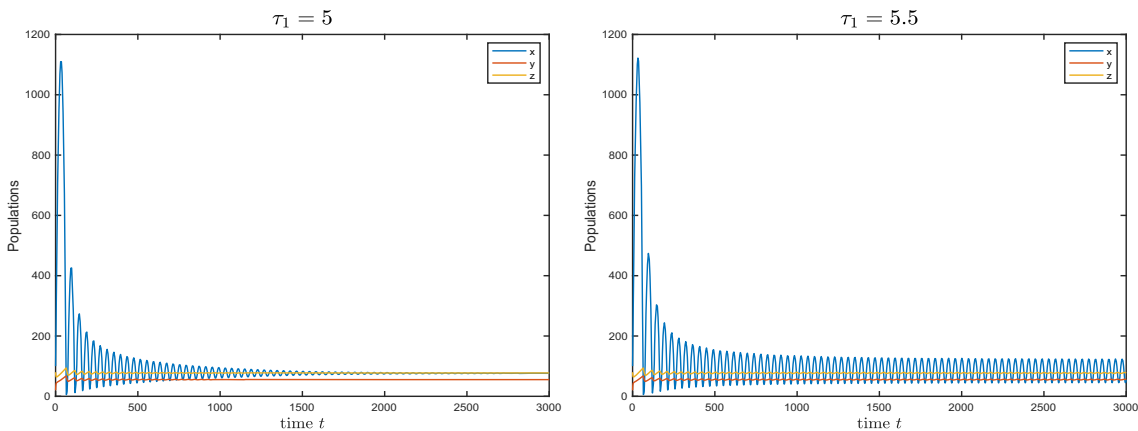

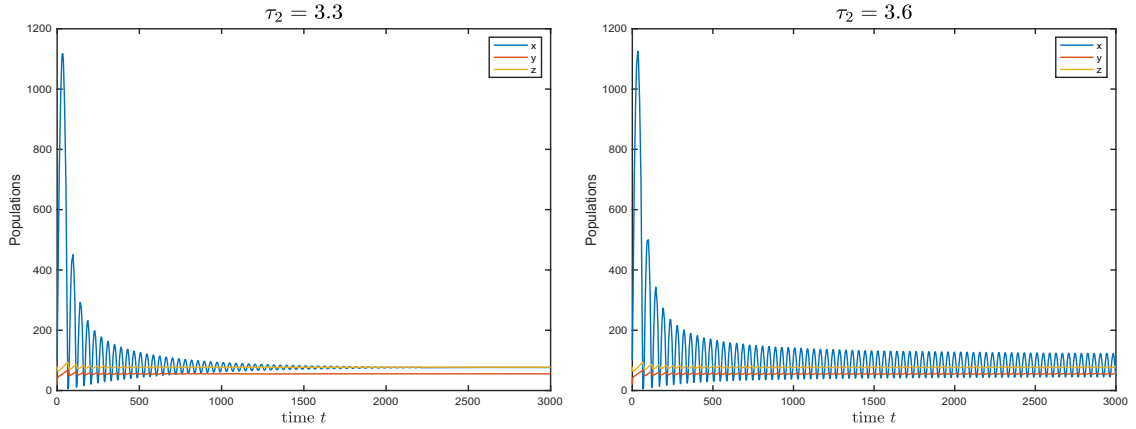**Figure 7:** Solution profiles for $\tau_1 > 0$, $\tau_2 = 0$.

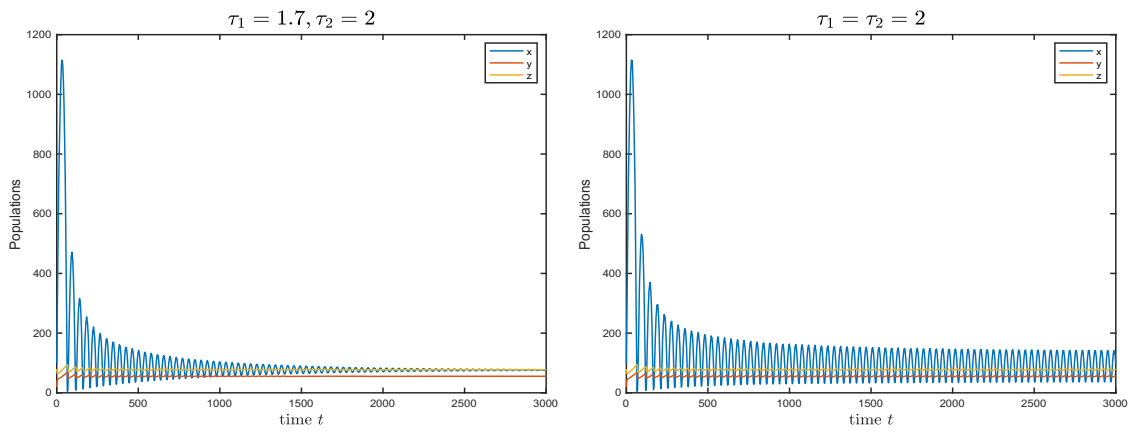**Figure 8:** Solution profiles for $\tau_1 = 0$, $\tau_2 > 0$.

Figure 9: Solution Profiles for τ_1, $\tau_2 > 0$.

susceptibles to COVID-19-infected diabetic and non-diabetic populations were $a_1 = 0.75$ and $b_1 = 0.5$, whereas in Example 2, we had $a_1 = 0.6$ and $b_1 = 0.6$. The exposure to the COVID-19 infection was same for both the populations in both the examples ($a = 2$, $b = 3$). In Example 1, we observed that the theoretical value of delay τ_1 (incubation period of COVID-19 infection in diabetic population) is 4.022, whereas in Example 2, we obtain $\tau_1 = 5.2$. This is due to the fact that in Example 2, less diabetic people are getting converted to the infected
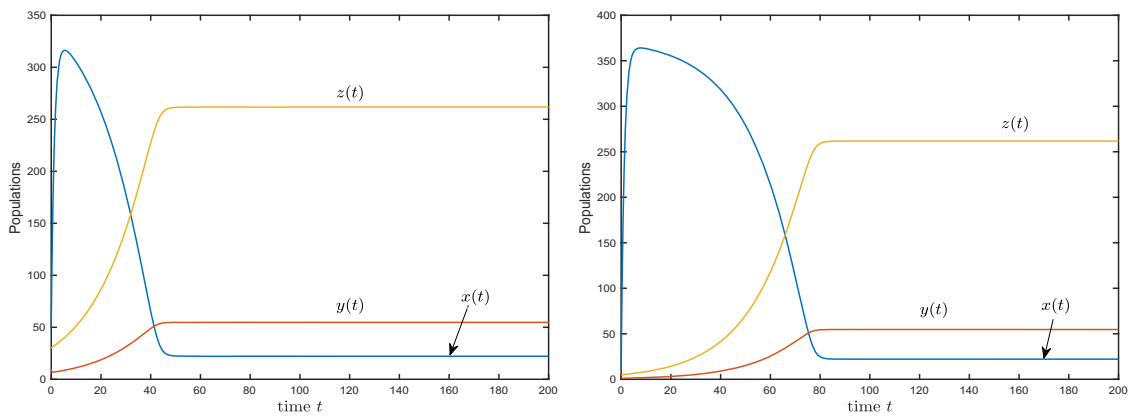

Figure 10: Solution profiles for $\tau_1 = \tau_2 = 0$ at different initial conditions.
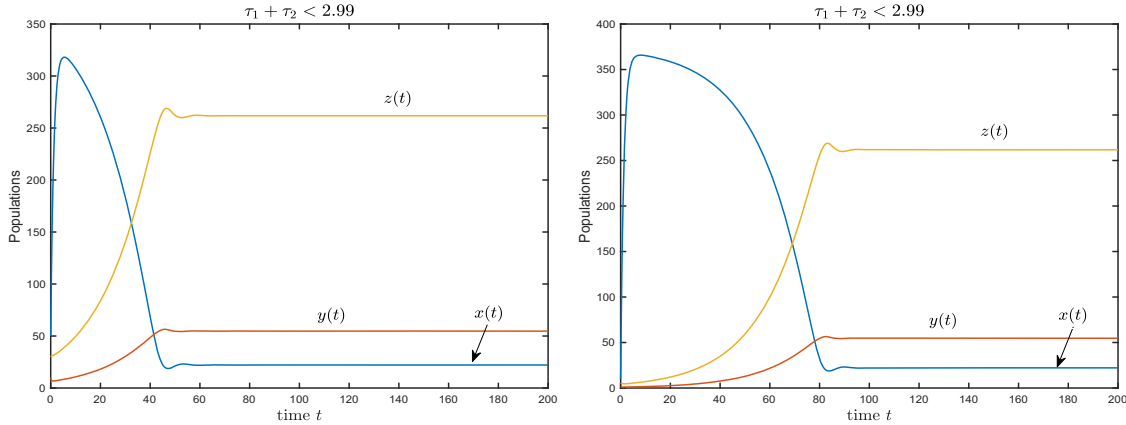
Figure 11: Corresponding solution profiles for τ_1, $\tau_2 > 0$ for different initial states.

population ($a_1 = 0.6$ as compared to $a_1 = 0.75$ in Example 1), and hence, their immunity is comparatively better, due to which the onset of symptoms is taking longer as compared to Example 1. Similarly, the delay $\tau_2 = 3.5$ in Example 2, as compared to $\tau_2 = 4.45$ in Example 1. This is again due to the fact that our conversion parameter b_1 in Example 1 is smaller (hence less people getting converted to infected population) as compared to Example 2. In Example 3, we showcased a scenario where the system will be globally stable for all initial populations irrespective of time delays, which is only possible if the treatment parameters (α_1 and α_2) are very high as compared to exposure rates (a and b) and conversion rates (a_1 and b_1). This is relevant to real-life scenario also. Example 3 illustrates the case where the system is globally stable, i.e. independent of initial states. Furthermore, these conditions are violated in Examples 1 and 2, implying that global and local stability need not go hand-in-hand usually. On the whole, our examples illustrate the results established and explain the contribution of parameters in stabilising or destabilising the system under the influence of time delays.

6 Conclusions and future work

In this article, we have focused on discussing the COVID-19 virus, which has emerged as the most prevalent and dangerous viral infection of this decade. Specifically, we have examined its impact on individuals who are diabetic, a chronic health condition that is currently widespread. To capture the real-life dynamics of the virus within the host's body, we have proposed a three-compartment model incorporating two time delays. These time delays have been introduced to enhance the model and represent the incubation period of the COVID-19 virus. We emphasize that ODE compartmental models do not adequately represent the transition of a susceptible individual to the infected compartment, as it is not an instantaneous process. Therefore, we have developed a delay compartmental model to better capture this aspect. In our study, we have conducted a local stability analysis of the model, where we derived upper bounds for the delay parameters τ_1 and τ_2. These bounds have been numerically verified in Section 5. Furthermore, we have performed a global stability analysis using a Lyapunov function. Finally, we have validated our theoretical findings through numerical experiments. We chose our model parameters in such a way that the incubation periods derived should be realistic. Numerous meta-analyses [34,36] estimate the incubation time of the COVID-19 virus to be around 5 days, with a range of 1.80–18.87 days. In particular, Wu et al. [36] provided incubation periods for different variants of the COVID-19 virus. From their meta-analysis of 141 articles, they found the incubation periods for the Alpha, Beta, Delta, and Omicron variants to be 5.00, 4.50, 4.41, and 3.42 days, respectively. These values closely align with the incubation periods obtained in our examples using synthetic data. Therefore, our model, with the chosen parameters, accurately reflects the real-life scenario.

We have emphasised on the incubation periods of the virus in populations; however, the treatment period is also of significant importance. Hence, a model with recovery or treatment delay is left for future endeavor.

Also, introduction of control/preventive measures such as vaccination or face mask usage in equation (2.1) could be an interesting study in the scenario of endemic prevalent conditions established here. Hence, we can further venture in this direction in our next studies. It is interesting to note that an increase in length of time delay in either of infected populations led to oscillations in susceptible population but has no impact on infected populations. This phenomenon needs to be explored further and verified with real-time environment. Authors noted that increase of lengths of time delays beyond the estimates obtained in the results leads only to disturb the stability of the endemic equilibrium leading a chaotic state. This is due to the fact that we have restricted our study to conditions of Lemma 3.1, which focuses only on non-changing of stability of the system, and parameters and functions are chosen to fit these conditions only. However, the existence of multiple bifurcation points and change of stability or instability status of the system are also interesting phenomena to explore for dynamical systems such as equation (2.1). We leave this for a future study.

References

[1]   Anand, M., Danumjaya, P., & Rao, P. R. S. (2023). A nonlinear mathematical model on the COVID-19 transmission pattern among diabetic and non-diabetic population. *Mathematics and Computers in Simulation*, *210*, 346–369.

[2]   Arshad, S., Siddique, I., Nawaz, F., Shaheen, A., & Khurshid, H. (2023). Dynamics of a fractional order mathematical model for COVID-19 epidemic transmission. *Physica A: Statistical Mechanics and its Applications*, *609*, 128383.

[3]   Barman, B., & Ghosh, B. (2019). Explicit impacts of harvesting in delayed predator-prey models. *Chaos Solitons Fractals*, *122*, 213–228.

[4]   Bhandari, S., Singh, A., Sharma, R., et al. (2020). Characteristics, treatment outcomes and role of hydroxychloroquine among 522 COVID-19 hospitalized patients in Jaipur City: An epidemio-clinical study. *Journal of the Association of Physicians of India*, *68*(6), 13–19.

[5]   Cariou, B., Wargny, M., Boureau, A. S., et al. (2022). Impact of diabetes on COVID-19 prognosis beyond comorbidity burden: the CORONADO initiative. *Diabetologia*, *65*, 1436–1449.

[6]   Cascella, M., Rajnik, M., Aleem, A., et al. *Features, evaluation, and treatment of coronavirus (COVID-19)* [Updated 2023 Jan 9].

[7]   Desoer, C., & Wang, Y. T. (1980). On the generalized Nyquist stability criterion. *IEEE Transactions on Automatic Control*, *25*(2), 187–196.

[8]   Ejaz, H., Alsrhani, A., Zafar, A., et al. (2020).COVID-19 and comorbidities: Deleterious impact on infected patients. *Journal of Infection and Public Health*, *13*(12), 1833–1839.

[9]   Freedman, H. I., & Sree Hari Rao, V. (1986). Stability criteria for a system involving two time delays. *SIAM Journal on Applied Mathematics*, *46*(4), 552–60.

[10] Ghosh, B., Barman, B., & Saha, M. (2023). Multiple dynamics in a delayed predator-Řprey model with asymmetric functional and numerical responses. *Mathematical Methods in the Applied Sciences*, *46*(5), 5187–5207.

[11] Gold, M. S., Sehayek, D., Gabrielli, S., et al. (2020). COVID-19 and comorbidities: A systematic review and meta-analysis. *Postgraduate Medicine*, *132*(8), 749–755.

[12] Grondelle, E. V., Bruggen, S. V., Rauh, S. P., et al. (2023). The impact of the covid-19 pandemic on diabetes care: the perspective of healthcare providers across Europe. *Primary Care Diabetes*, *17*(2), 141–147.

[13] Hale, J. K. (1977). *Theory of Functional Differential Equations*, 2nd Edition, New York: Springer.

[14] Hertz, D., Jury, E. I., & Zeheb, E. (1984). Simplified analytic stability test for systems with commensurate time delays. *IEE Proceedings - Control Theory and Applications*, *131*(1), 52–56.

[15] Jeong, I. K., Yoon, K. H., & Lee, M. K. (2020). Diabetes and COVID-19: Global and regional perspectives. *Diabetes Research and Clinical Practice*, *166*, 108303.

[16] Joshi, S. C., & Pozzilli, P. (2022). COVID-19 induced Diabetes: A novel presentation. *Diabetes Research and Clinical Practice*, *191*, 110034.

[17] Kalmanovskii, V. B., & Nosov, V. R. (1986). *Stability of Functional Differential Equations*, London: Academic Press.

[18] Khan, M. S., Samreen, M., Ozair, M., et al. (2021). Bifurcation analysis of a discrete-time compartmental model for hypertensive or diabetic patients exposed to COVID-19. *The European Physical Journal*, *136*(8), 853.

[19] Khunti, K., Aroda, V. R., Aschner, P., Chan, J. C. N., et al. (2022). The impact of the COVID-19 pandemic on diabetes services: planning for a global recovery. *The Lancet Diabetes & Endocrinology*, *10*(12), 890–900.

[20] Kouidere, A., Youssoufi, L. E., Ferjouchia, H., et al. (2021). Optimal Control of Mathematical modeling of the spread of the COVID-19 pandemic with highlighting the negative impact of quarantine on diabetics people with Cost-effectiveness. *Chaos, Solitons & Fractals*, *145*, 110777.

[21] Kretzschmar, M., & Wallinga, J. (2009). Mathematical models in infectious disease epidemiology. *Modern Infectious Disease Epidemiology*, *28*, 209–21.

[22] Lai, H., Yang, M., Sun, M., et al. (2022). Risk of incident diabetes after COVID-19 infection: A systematic review and meta-analysis. *Metabolism*, *137*, 155330.

[23] Ng, K. Y., & Gui, M. M. (2020). COVID-19: Development of a robust mathematical model and simulation package with consideration for ageing population and time delay for control action and resusceptibility. *Physica D: Nonlinear Phenomena*, *411*, 132599.

[24] Okyere, S., & Ackora-Prah, J. (2022). A mathematical model of transmission dynamics of SARS-CoV-2 (COVID-19) with an underlying condition of diabetes. *International Journal of Mathematics and Mathematical Sciences*, *2022*, 7984818.

[25] Overton, C. E., Stage, H. B., Ahmad, S., et al. (2020). Using statistics and mathematical modelling to understand infectious disease outbreaks: COVID-19 as an example, *Infectious Disease Modelling*, *5*, 409–441.

[26] Özköse, F., & Yavuz, M. (2022). Investigation of interactions between COVID-19 and diabetes with hereditary traits using real data: A case study in Turkey. *Computers in Biology and Medicine*, *141*, 105044.

[27] Rao, P. R. S., & Kumar, M. N. (2015). A dynamic model for infectious diseases: The role of vaccination and treatment. *Chaos Solitons & Fractals*, *75*, 34–49.

[28] Rizvi, A. A., Kathuria, A., Mahmeed, W. A., Al-Rasadi, K., et al. (2022). Post-COVID syndrome, inflammation, and diabetes. *Journal of Diabetes and its Complications*, *36*(11), 108336.

[29] Sanyaolu, A., Okorie, C., Marinkovic., A., et al. (2020). Comorbidity and its Impact on Patients with COVID-19. *SN Comprehensive Clinical Medicine*, *2*, 1069–1076.

[30] Sathish, T., Kapoor, N., Cao, Y., Tapp, R. J., & Zimmet, P. (2021). Proportion of newly diagnosed diabetes in COVID-19 patients: A systematic review and meta-analysis. *Diabetes, Obesity and Metabolism*, *23*(3), 870–874.

[31] Singh, H. P., Bhatia, S. K., Bahri, Y., & Jain, R. (2022). Optimal control strategies to combat COVID-19 transmission: A mathematical model with incubation time delay. *Results in Control and Optimization*, *9*, 100176.

[32] Song, H., Wang, R., Liu, S., Jin, Z., & He, D. (2022). Global stability and optimal control for a COVID-19 model with vaccination and isolation delays. *Results in Physics*, *42*, 106011.

[33] Ssebuliba, J., Nakakawa, J. N., Ssematimba, A., & Mugisha, J. Y. T. (2022). Mathematical modelling of COVID-19 transmission dynamics in a partially comorbid community. *Partial Differential Equations in Applied Mathematics*, *5*, 100212.

[34] Stephen, A. L., Kyra, H. G., Qifang, B., et al. (2020). The incubation period of coronavirus disease 2019 (COVID-19) from publicly reported confirmed cases: estimation and application. *Annals of Internal Medicine*, *172*(9), 577–582.

[35] Unnikrishnan, R., & Misra, A. (2021). Diabetes and COVID19: a bidirectional relationship. *Nutrition & Diabetes*, *11*(11), 21.

[36] Wu, Y., Kang, L., Guo, Z., Liu, J., et al. (2022). Incubation period of COVID-19 caused by unique SARS-CoV-2 strains: A systematic review and meta-analysis. *JAMA Network Open*, *5*(8), e2228008.

[37] WHO Coronavirus (COVID-19) Dashboard, https://covid19.who.int/.